Quantum ignition of deflagration in the Fe_8 molecular magnet

Tom Leviant and Amit Keren
Department of Physics, Technion–Israel Institute of Technology, Haifa 32000, Israel

Eli Zeldov and Yuri Myasoedov
Department of Condensed Matter Physics, The Weizmann Institute of Science, 76100 Rehovot, Israel
(Received 4 August 2014; revised manuscript received 23 September 2014; published 8 October 2014)

We report spatially resolved, time-dependent, magnetization reversal measurements of an Fe_8 single molecular magnet using a microscopic Hall bar array. We found that a deflagration process, where molecules reverse their spin direction along a moving front, can be ignited quantum mechanically ($T \to 0$) at a resonance field, with no phonon pulse. The avalanche front velocity is of the order of 1 m/s and is sensitive to field gradients and sweep rates. We also measured the thermal diffusivity κ in Fe_8. This allows us to estimate the "flame" temperature.

DOI: 10.1103/PhysRevB.90.134405 PACS number(s): 75.50.Xx, 45.70.Ht, 75.45.+j, 75.60.Ej

I. INTRODUCTION

Single molecular magnets (SMMs) are an excellent model system for the study of macroscopic quantum phenomena and their interplay with the environment. In recent years, the focus of these studies shifted from single molecule to collective effects. While there are two famous SMMs that show quantum behavior, namely, Fe_8 and Mn_{12}, most of the work on collective effects has been focused on Mn_{12}. Indeed, in Mn_{12} intriguing effects were found, such as deflagration [1,2], quantum assisted deflagration [3], and detonation [4]. In all these cases, a spin reversal front propagates through the sample as deflagration. Although showing some signs of quantum behavior [3], these processes are assisted by phonons generated by a heat pulse [5] or surface acoustic waves [6]. Here, we focus on the magnetic deflagration phenomena in Fe_8, where pure quantum effects exist below 400 mK.

We find that it is possible to ignite the deflagration in the quantum regime by sweeping the external magnetic field through the matching field, without any phonon assistance. In addition, we measure the deflagration velocity V_d for various sweep rates and applied field gradients. The sweep rate parameter is not part of current deflagration theories [7]. The gradient is expected to affect the ignition threshold [7], but its effect on the speed of deflagration still needs to be addressed. We also determine the thermal diffusivity κ and predict the temperature of the spin reversal front, known as the flame temperature T_f. This prediction could be used to search for cold deflagration [8].

The Fe_8 SMM has a spin $S = 10$ ground state, as does Mn_{12}. The magnetic anisotropy corresponding to an energy barrier between the spin projection quantum number $m = \pm 10$ and $m = 0$ is 29.2 K [9–13]; in Mn_{12} this anisotropy is 70 K [14,15]. Fe_8 molecules show temperature-independent hysteresis loops in the quantum regime, with magnetization jumps at matching fields that are multiples of 0.225 T [16,17]. However, when tunneling is taking place from state m to m', where $|m'| \neq 10$, the excited state can decay to the ground state $|m'| = 10$, releasing energy in the process. In a macroscopic sample, this energy release can increase the temperature and support a deflagration process by assisting the spin flips. Spontaneous deflagration in Mn_{12} takes place at various and not necessarily matching fields higher than 1 T. The deflagration velocity starts from 1 m/s and increases with an increasing (static) field up to 15 m/s [1].

II. MAGNETIC DEFLAGRATION IN Fe_8

Our deflagration velocity measurements are based on local and time-resolved magnetization detection using a Hall sensor array.

A. Experimental details

The array is placed at the center of a magnet and gradient coils. A schematic view of the array and coils is shown in the inset of Fig. 1. The array is consists of Hall bars of dimensions 100×100 μm^2 with 100 μm intervals; the active layer in these sensors is a two-dimensional electron gas formed at the interface of GaAs/AlGaAs heterostructures. The Hall sensor array resides in the center of a printed circuit board (PCB). There is a hole in the PCB and the Hall sensor is glued directly on a copper plate cold finger, which extends from the dilution refrigerator (DR) mixing chamber. Gold wire bonding connects the sensors and the leads on the PCB. All wires are thermally connected to the mixing chamber. The surface of the Hall sensors is parallel to the applied field. Consequently, the effect of the applied field on the sensor is minimal and determined only by the ability to align the array surface and field. The sample and sensors are cooled to 100 mK using a DR. The array backbone has a resistance of 3–4 kΩ at our working temperatures, and is excited with a 10 μA dc current. No effect of the sensors' excitation on the DR-mixing chamber temperature was detected. The Hall voltage from each sensor is filtered with a 30 Hz low-pass filter for hysteresis measurements and a 200 Hz high-pass filter for the deflagration measurements. The voltage is amplified 500 times by a differential amplifier. It is digitized with an NI USB 6251 A/D card at a rate of 50 Hz and 20 kHz for the hysteresis and deflagration measurements, respectively.

A magnetic field gradient can also be produced by two superconducting coils wound in the opposite sense. They are placed at the center of the main coil and produce 0.14 mT/mm per ampere. Since there is no option of adjusting the sample position after it has been cooled, it is reasonable to assume that the sample is not exactly in the center of the main magnet. In

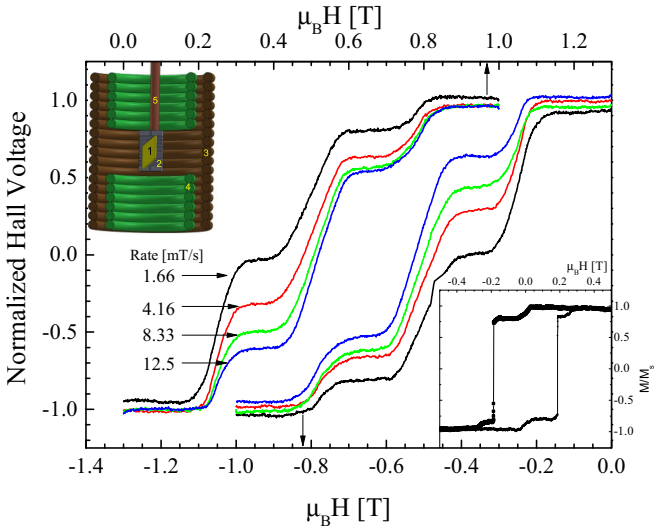

FIG. 1. (Color online) Fe_8 hysteresis loops for a sample that does not show avalanches at different magnetic field sweep rates. The magnetization is measured via one Hall sensor of the array. The fields for the positive sweep rates are given by the bottom x axis, and for the negative sweep rates by the top x axis. The upper inset shows the experimental setup including (1) sample, (2) Hall sensor array, (3) main coils, (4) gradient coils, and (5) cold finger leading to the dilution refrigerator mixing chamber. The lower inset shows the hysteresis loop for a sample that does experience avalanches. Only two magnetization steps are observed in this case.

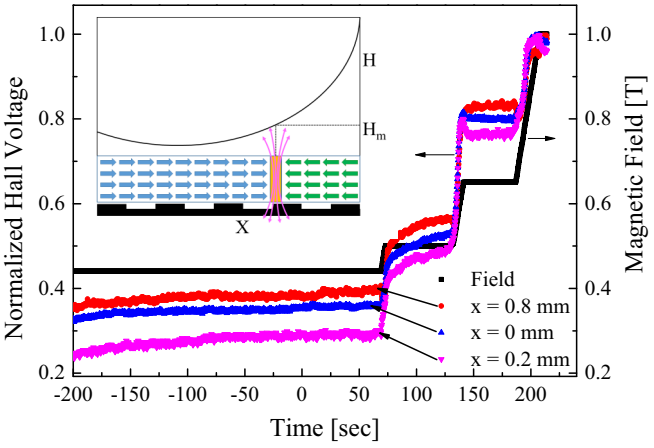

FIG. 2. (Color online) Magnetization as a function of time for a sample of the first type with no avalanche. The magnetization is measured via three different Hall sensors. The field is swept discontinuously. The solid (black) line shows the field value as a function of time on the right y axis. The magnetization, presented on the left y axis, changes only when the field changes. The inset demonstrates a tunneling front evolution in a case where the matching field H_m moves across the sample during a sweep. H is an instantaneous field intensity. It changes with time and varies in space. The tunneling region with mixed up and down spin has zero magnetization. The expelled magnetic induction **B** is detected by the Hall sensors.

addition, the sample has corners and edges. Therefore, a field gradient is expected even when the gradient coils are turned off.

Typical sample dimensions are $3 \times 2 \times 1$ mm^3. The samples have clear facets and are oriented with the easy axis parallel to the applied field. They are covered by a thin layer of superglue and placed directly on the surface of the Hall sensor with Apiezon-N grease, which is used to protect the sample from disintegration and hold it in place.

In the experiments, the molecules are polarized by applying a magnetic field of ± 1 T in the easy axis direction $\hat{\mathbf{z}}$. Afterwards, the magnetic field is swept to ∓ 1 T. The sweep is done at different sweep rates and under various applied magnetic field gradients. During the sweep, the amplified Hall voltage from all sensors and the external field are recorded. From the raw field-dependent voltage of each sensor, a straight line is subtracted. This line is due to the response of the Hall sensor to the external field. The line parameters are determined from very high and very low fields where no features in the raw data are observed.

B. Results

We found that Fe_8 samples can be divided into two categories: those that do not show deflagration, which have multiple magnetization steps regardless of the sweep rate, and those that show deflagration where the number of magnetization steps depends on the sweep rate. In Fig. 1, we present the normalized Hall voltage as detected by one of the Hall sensors from a sample of the first category. The normalization is by the voltage at a field of 1 T where the molecules are fully polarized. Thus, the normalized voltage provides M/M_0, where M is the magnetization and M_0 is the saturation magnetization. The bottom abscissa is for a sweep where the field decreases from 1 T. The top abscissa is for a sweep where the field increases from -1 T. The magnetization shows typical steps at intervals of 0.225 T. No step is observed near zero field. In addition, the hysteresis loop's coercivity increases as the sweep rate increases. These results are in agreement with previous measurements on Fe_8 [17]. They are presented here to demonstrate that the Hall sensors are working properly, that their signals indeed represent the Fe_8 magnetization, and that in some samples all magnetization steps are observed.

The hysteresis loop of a sample from the second category is plotted in the bottom inset of Fig. 1. In this case, there is a small magnetization jump at zero applied field, followed by a nearly full magnetization reversal at a field of 0.2 T in the form of deflagration. This kind of spontaneous, full magnetization reversal is found in various kinds of magnets [18]. However, in all Fe_8 samples tested in this and other experiments in our group [19], deflagration occurred only at the first matching field. We could not tell in advance whether a sample was of the first or second category. We always worked with samples of approximately the same dimensions. This is in contrast to Mn_{12}, where deflagration is associated with large samples [7].

The deflagration velocity measurements in Fe_8 should be done with extra care. In deflagration there is, of course, a propagating front where spins flip. But since our measurements in Fe_8 are done by sweeping the field through resonance, there is a similar front even without deflagration. This is demonstrated in the inset of Fig. 2. In this inset, a sample

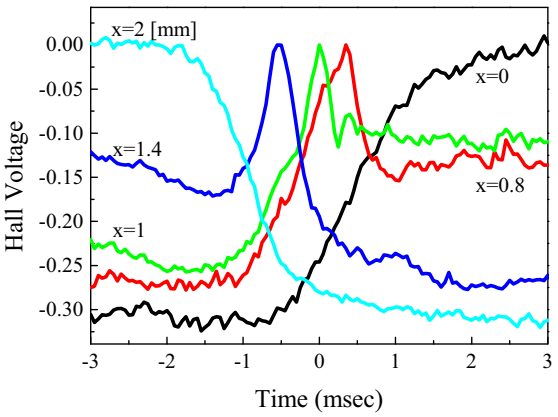

FIG. 3. (Color online) Hall voltage as a function of time for each of the sensors on the array for a sample that has avalanches (as in the inset of Fig. 2). The voltage from each sensor shows a peak or a cusp at different times. The evolution of the peaks and cusps provides the avalanche propagation velocity.

placed off the symmetry point of a symmetric field profile is shown. Thus, the sample experiences a field gradient. Due to this gradient, tunneling of molecules will start first at a particular point in the sample where the local field is at a matching value. The spin reversal front will then propagate from that point to the rest of the sample as the external field is swept. In this case, pausing the field sweep will stop the magnetization evolution.

This is demonstrated in Fig. 2 for a deflagration-free sample. The left ordinate is the normalized Hall voltage (solid symbols) from three different sensors on the array. Each symbol represents a different sensor. The right ordinate is the applied magnetic field (line). The voltage and field are plotted as a function of time. We focus on fields before, near, and after the third transition in Fig. 1. For the most part, the magnetization changes only when the field changes, even in the middle of a magnetization jump. This means that the sample is subjected to some field gradients and a tunneling front propagates through the sample even without deflagration. It is possible to estimate the matching field front velocity as $V_m \sim 1.5 \times 10^{-4}$ m/s from a typical transition width (0.1 T), a typical sweep rate (5 mT/s), and the sample length (3 mm).

In Fig. 3, we zoom in on the magnetization jump of samples from the second category at a 0.2 T field. In this figure, we show the time-resolved Hall voltage from five different sensors along the array. The three middle sensors show a peak in the Hall voltage, which is experienced by each sensor at different times. The two outer sensors experience a smoother variation of the Hall voltage, in the form of cusps, also at different times. This type of behavior is a clear indication of a magnetization reversal front propagating from one side of the sample to the other. The peaks and cusps are due to a zero magnetization front, where the magnetization **M** changes sign due to tunneling. At the same front, the magnetic induction **B** from the sample is forced to point outward and toward the sensors, to maintain zero divergence [20]. The field configuration is also demonstrated in the inset of Fig. 2. By following the time evolution of the peaks and cusps, we can determine the front velocity. Since the sensors are spaced by

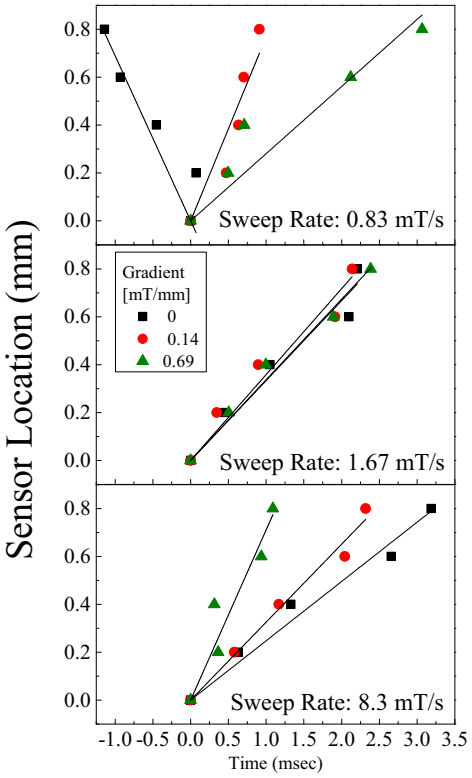

FIG. 4. (Color online) Sensor position as a function of time at which a peak or cusp in the Hall voltage appears for three different sweep rates and three different magnetic field gradients. The slope of each line gives the avalanche velocity.

parts of a millimeter and the peaks are spaced by parts of a millisecond, the deflagration velocity V_d is of the order of 1 m/s, which is much higher than V_m.

We found that the deflagration propagation direction and velocity can be affected by applying field gradients as long as the sweep rate is low. This is demonstrated in Fig. 4. In this figure, we show for each detector location the time at which it experiences a peak or a cusp. The slope of each line is the deflagration velocity. For the lowest sweep rate of 0.83 mT/s with no gradient, the velocity is negative. It becomes positive as the gradient is switched on to 0.14 mT/mm, but becomes slower as the gradient increases to 0.69 mT/mm. Reversal of deflagration direction, but with constant velocity magnitude, was found also in Mn_{12} by moving the sample along the main magnet axis [21]. The effect of the gradient is opposite and weaker for our highest sweep rate of 8.3 mT/s. In this case, all velocities are positive and increase as the gradient increases. Only at the intermediate sweep rate of 1.67 mT/s does the gradient have no effect on the velocity. Although we find it challenging to explain the gradient dependence of the deflagration velocity, we do learn from this experiment that the safest sweep rate from which one can estimate the deflagration velocity is around 2 mT/s. In this case, the external gradient does not affect the velocity.

The ratio between sweep rates and gradient (when it is on) is a quantity with units of velocity of the order of tens of millimeters per second. This is much lower than V_d. Therefore, the gradient experiment is another indication, but

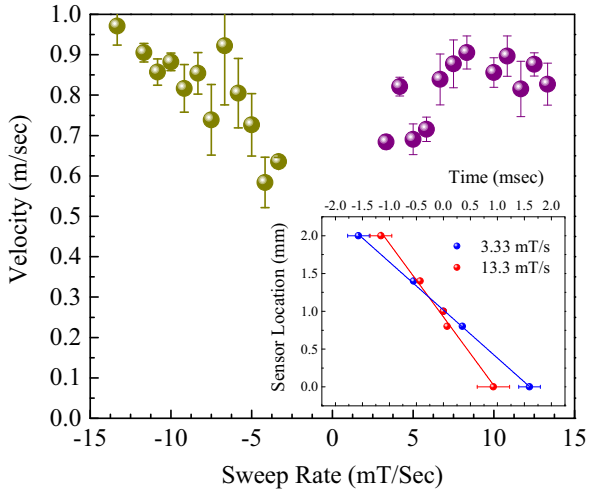

FIG. 5. (Color online) Avalanche velocity as a function of magnetic field sweep rate at zero gradient. The field is swept from positive to negative and vice versa. For sweep rates slower than 3 mT/s, no avalanche was observed in this sample. The inset shows raw data of peak position vs time for two different sweep rates.

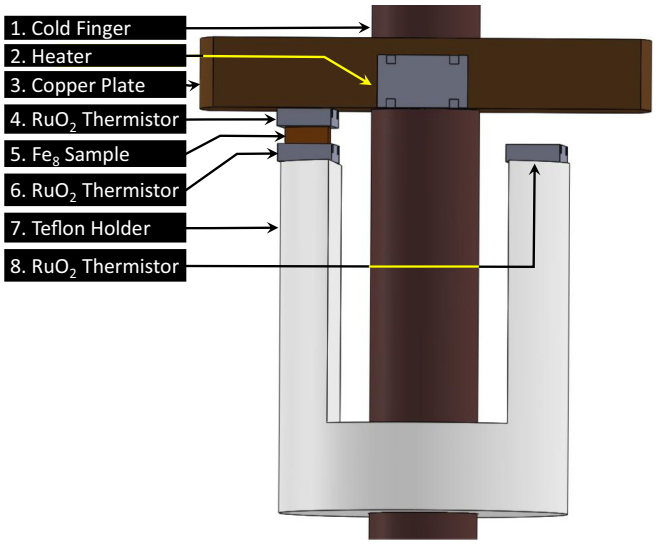

FIG. 6. (Color online) Thermal diffusivity experimental setup. The heat pulse is provided by heater 2. Thermistor 4 measures $T_{\rm hs}$ and thermistor 6 measures $T_{\rm cs}$. Thermistor 8 is used to determine heat leaks via the measurement wires.

with a deflagrating sample, that the propagation of the external magnetic field does not determine the deflagration velocity, and that V_d is an internal quantity of the molecules. In addition, a gradient-dependent V_d is not explained at present by magnetic deflagration theory.

Finally, in Fig. 5 we depict V_d as a function of sweep rate with zero applied gradient. The field was swept from positive to negative and vice versa. The sample used in this experiment was of the second category and produced deflagration only for sweep rates higher than 3 mT/s. Slower sweep rates generated the usual magnetization jumps, as shown in Fig. 1. Although there is some difference between the velocity for different sweep directions, it is clear that the velocity tends to increase with increasing sweep rate, and perhaps saturate. This is demonstrated with raw data in the inset of Fig. 5. The theory of magnetic deflagration [7] does not account for sweep-rate-dependent ignition, or deflagration velocities [1,3]. In light of the gradient experiment, the most representative deflagration velocity for Fe_8 is $V_d = 0.6$ m/s.

III. THERMAL DIFFUSIVITY IN Fe_8

To clarify the role of heat propagation in the deflagration process of Fe_8, we also measured the thermal diffusivity κ between 300 mK and 1 K.

A. Experimental details

The thermal diffusivity measurements were performed using two thermistors mounted on opposite sides of the sample and a heater on the hot side of the sample. This configuration is shown in Fig. 6. The hot side is attached to the cold finger and is hot only after the heat pulse. The thermometers are RuO_2 films. The heater is a 2.2 kΩ resistor. The hot side thermistor is between the heater and the sample. The cold side thermistor is between the sample and a Teflon plate. It has a weak thermal link to the cold plate via the measurement wires only. A heat pulse is generated by applying 8 V to the 2.2 kΩ resistor for a duration of $\Delta t_h = 1$ ms using a function generator, which also gives the trigger for the RuO_2 voltage measurement. From the RuO_2 voltage, the time-dependent temperatures of the hot side ($T_{\rm hs}$) and of the cold side ($T_{\rm cs}$) are extracted. The system has been tested by repeating the measurement without the sample to ensure that the recorded heat on the cold side flows through the sample and not through the wires.

B. Results

The normalized changes in $T_{\rm hs}$ and $T_{\rm cs}$ are shown in Fig. 7. The thermal diffusivity is defined via the heat equation

$$\frac{\partial T}{\partial t}(x,t) - \kappa \frac{\partial^2 T(x,t)}{\partial x^2} = 0,$$

where $T(x,t)$ is the location- and time-dependent temperature along the sample. For a long rod $\sqrt{\Delta t_h \kappa} \ll l$, one has that

$$\Delta T_{\rm cs}(t) = c \int_0^t \frac{x \exp\left(-\frac{x^2}{4k(t-s)}\right)}{(4\pi\kappa)^{1/2}(t-s)^{3/2}} \Delta T_{\rm hs}(s) ds.$$

We fit this expression to our $T_{\rm cs}(t)$ data with c and κ as fit parameters. c accounts for the coupling of the two thermometers to the sample. The fit is shown by the solid line in Fig. 7. Although the fit is not perfect, it does capture the data quite well. The κ obtained with this method at a few different temperatures is depicted in the inset of Fig. 7. At the lower temperature it measured $\kappa = 2 \times 10^{-6}$ m^2/s. κ and Δt_h obey the long rod condition. It is much smaller than κ of Mn_{12}, which is estimated to be $\kappa = 10^{-5} - 10^{-4}$ m^2/s [1,22].

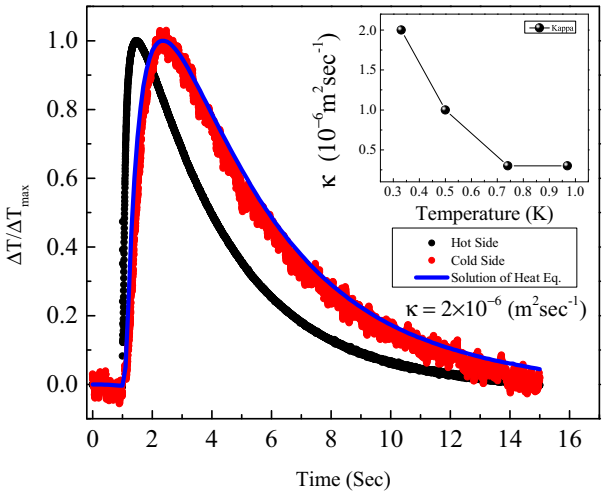

FIG. 7. (Color online) Normalized relative temperature as a function of time at two sides of the sample. The solid line is a solution of the heat equation for $\kappa = 2 \times 10^{-6}$. The inset shows thermal diffusivity κ at different temperatures.

We are now in a position to estimate the flame temperature using the equation [1]

$$V_d = \sqrt{\frac{k}{\tau_0}} \exp\left(\frac{-U}{2k_B T_f}\right). \quad (1)$$

We use $\tau_0 = 3.4 \times 10^{-8}$ s and $U = 24.5$ K from the Fe_8 magnetization relaxation measurements of Ref. [23]. Equation (1) gives $T_f = 4.8$ K. This is very similar to the energy difference between consecutive states at the bottom of the well of Fe_8 at the first matching field, which is 4.86 K. An increase in the sample temperature during deflagration was indeed reported in Ref. [19], but with a thermometer connected to the mixing chamber. Measuring T_f properly, with a thermometer attached to the sample, could serve as a strong test of the theory of magnetic deflagration in the Fe_8 molecular magnets.

IV. DISCUSSION

Our experiments show that the deflagration process in Fe_8 propagates at a velocity very similar to deflagration in Mn_{12}, but has a few different features: It can be ignited (in some samples) at $T \to 0$ by tunneling simply by sweeping fast through a matching field. The velocity increases with increasing sweep rate. This is surprising since at high sweep rates fewer molecules tunnel at the ignition site, the initial flame should be colder, and the velocity slower. On the other hand, the velocity variation could be due to increasing average field during the deflagration with increasing sweep rate. Increasing field means increasing T_f. However, within $\sim$1 ms of deflagration, the field changes by $\sim$1 mT due to the sweep, which is too small to cause a noticeable variation in V_d. The velocity is also sensitive to a small gradient of $\sim$1 mT across the sample. This indicates extreme sensitivity to the resonance condition. It is intriguing how at a flame temperature of 5 K, when normally magnetization steps are not observed, the system is so sensitive to the sweep rate or resonance conditions.

ACKNOWLEDGMENT

This study was partially supported by the Russell Berrie Nanotechnology Institute, Technion, Israel Institute of Technology.

[1] Y. Suzuki, M. P. Sarachik, E. M. Chudnovsky, S. McHugh, R. Gonzalez-Rubio, N. Avraham, Y. Myasoedov, E. Zeldov, H. Shtrikman, N. E. Chakov, and G. Christou, Phys. Rev. Lett. **95**, 147201 (2005).

[2] P. Subedi, S. Vélez, F. Maciá, S. Li, M. P. Sarachik, J. Tejada, S. Mukherjee, G. Christou, and A. D. Kent, Phys. Rev. Lett. **110**, 207203 (2013).

[3] A. Hernández-Minguez, J. M. Hernandez, F. Macià, A. García-Santiago, J. Tejada, and P. V. Santos, Phys. Rev. Lett. **95**, 217205 (2005).

[4] W. Decelle, J. Vanacken, V. V. Moshchalkov, J. Tejada, J. M. Hernández, and F. Macià, Phys. Rev. Lett. **102**, 027203 (2009); M. Modestov, V. Bychkov, and M. Marklund, *ibid.* **107**, 207208 (2011); D. A. Garanin and S. Shoyeb, Phys. Rev. B **85**, 094403 (2012); D. A. Garanin, *ibid.* **88**, 064413 (2013).

[5] S. McHugh, R. Jaafar, M. P. Sarachik, Y. Myasoedov, A. Finkler, H. Shtrikman, E. Zeldov, R. Bagai, and G. Christou, Phys. Rev. B **76**, 172410 (2007).

[6] F. Macià, A. Hernández-Mínguez, G. Abril, J. M. Hernandez, A. García-Santiago, J. Tejada, F. Parisi, and P. V. Santos, Phys. Rev. B **76**, 174424 (2007).

[7] D. A. Garanin and E. M. Chudnovsky, Phys. Rev. B **76**, 054410 (2007); D. A. Garanin, in *Molecular Magnets*, edited by J. Bartolomé *et al.*, Springer Series in NanoScience and Technology Vol. 41 (Springer, Berlin, 2014).

[8] D. A. Garanin and E. M. Chudnovsky, Phys. Rev. Lett. **102**, 097206 (2009); D. A. Garanin, Phys. Rev. B **80**, 014406 (2009).

[9] W. Wernsdorfer and R. Sessoli, Science **284**, 133 (1999).

[10] A. Mukhin, B. Gorshunov, M. Dressel, C. Sangregorio, and D. Gatteschi, Phys. Rev. B **63**, 214411 (2001).

[11] A.-L. Barra, P. Debrunner, D. Gatteschi, Ch. E. Schulz, and R. Sessoli, Europhys. Lett. **35**, 133 (1996).

[12] R. Caciuffo, G. Amoretti, A. Murani, R. Sessoli, A. Caneschi, and D. Gatteschi, Phys. Rev. Lett. **81**, 4744 (1998).

[13] K. Park, M. A. Novotny, N. S. Dalal, S. Hill, and P. A. Rikvold, Phys. Rev. B **66**, 144409 (2002).

[14] A. Caneschi, D. Gatteschi, R. Sessoli, A. L. Barra, L. C. Brunel, and M. Guillot, J. Am. Chem. Soc. **113**, 5873 (1991).

[15] R. Sessoli, H.-L. Tsai, A. R. Schake, S. Wang, J. B. Vincent *et al.*, J. Am. Chem. Soc. **115**, 1804 (1993).

[16] W. Wernsdorfer, R. Sessoli, A. Caneschi, D. Gatteschi, A. Cornia, and D. Mailly, J. Appl. Phys. **87**, 5481 (2000).

[17] A. Caneschi, D. Gatteschi, C. Sangregorio, R. Sessoli, L. Sorace, A. Cornia, M. A. Novak, C. Paulsen, and W. Wernsdorfer, J. Magn. Magn. Mater. **200**, 182 (1999).

[18] R. Mahendiran, A. Maignan, S. Hébert, C. Martin, M. Hervieu, B. Raveau, J. F. Mitchell, and P. Schiffer, Phys. Rev. Lett. **89**, 286602 (2002); S. Velez, J. M. Hernández, A. Fernandez, F. Macià, C. Magen, P. A. Algarabel, J. Tejada, and E. M. Chudnovsky, Phys. Rev. B **81**, 064437 (2010).

[19] T. Leviant, S. Hanany, Y. Myasoedov, and A. Keren, Phys. Rev. B **90**, 054420 (2014).

[20] J. R. Friedman and M. P. Sarachik, Annu. Rev. Condens. Matter Phys. **1**, 109 (2010).

[21] A. Hernández-Mínguez, F. Macià, J. M. Hernandez, J. Tejada, L. H. He, and F. F. Wang, Europhys. Lett. **75**, 811 (2006).

[22] J. M. Hernández, P. V. Santos, F. Macià, A. García-Santiago, and J. Tejada, Appl. Phys. Lett. **88**, 012503 (2006).

[23] C. Sangregorio, T. Ohm, C. Paulsen, R. Sessoli, and D. Gatteschi, Phys. Rev. Lett. **78**, 4645 (1997).